Capacity assessment of multi-storey RC walls

1° *fib* Italy Symposium on Concrete and Concrete Structures

<u>Paper template</u>

Capacity assessment of multi-storey RC walls

Francesca Vecchi and Beatrice Belletti

Department of Engineering and Architecture,
University of Parma,
Parco Area delle Scienze 181/A, 43124, Parma (ITALY)

Abstract

Phase 2 of the CASH benchmark was dedicated to the response prediction of multi-storey reinforced concrete (RC) walls used as seismic resisting members in nuclear power plants. Nonlinear static and dynamic analyses have been carried out to check the reliability of non-linear finite element analysis (NLFEA) to assess the seismic capacity of reinforced concrete walls. Authors attended the benchmark by modelling RC walls using multi-layered shell elements and by adopting a self implemented crack model. The paper describes modelling strategies and some critical issues of the Eurocode 8 prescriptions for the shear demand and shear capacity evaluation of multi-storey RC walls.

1 Introduction

Nonlinear finite element analysis (NLFEA) is a more and more used tool in engineering practice for the structural response prediction. The NLFEA trustworthiness must be verified by means of comparisons with experimental test and via benchmark experiences. Indeed, the reliability of response predictions assisted by numerical simulation, depends both on the analyst capability to set up an appropriate modelling of the structure and the facilities of the adopted software. Certainly the result of NLFEAs is strongly influenced by the models implemented for the nonlinear prediction of the material behaviors. For this reason, a fixed crack model, called PARC_CL 2.1 [1]-[2], for reinforced concrete (RC) elements subjected to cyclic and dynamic loadings was implemented at the University of Parma as a user subroutine in the software ABAQUS [3].

The PARC_CL 2.0 has been validated by means the comparison with experimental results and during numerous international benchmarks. In particular, in the context of the response prediction of RC wall system, the University of Parma attented ConCrack2 [4], SMART-2013 [5], CASH [6]. This paper reports the results obtained on the international benchmark CASH-phase 2 organized by OEDC-NEA (Nuclear Energy Agency) [7]. The main objective of the CASH benchmark was the evaluation not only of the reliability of finite element commercial software but also of the ability, in current engineer practice, to calculate the resistance of RC walls subjected to various seismic loading.

During the CASH-phase 2 participants carried out pushover, cyclic and dynamic analyses to assess the capacity of full scale RC walls extracted from a nuclear power plants (NPP) building subjected to various seismic loading intensities. 9 teams participated at the benchmark, using both commercial software (ATHENA, ABAQUS, SOFISTIK, SOLVIA, Ls-Dyna) and open access software (CAST3M, Aster, VecTor2). NLFEA have been carried out using plasticity based model or crack models available in the software material libraries; only the team from the University of Toronto and the team from the University of Parma adopted crack models self-implemented in user subroutines. Finally, during the workshop held in June 2017, the results obtained from various teams coming from academia, industry and nuclear research organizations showed that the predictions of about a half of the participants were in good agreement. During the workshop the results obtained from the University of Parma were in good agreement with the results obtained by the majority of the partecipants, confirming the validity of the adopted numerical model.

The CASH-phase 2 was organized in three different tasks with increasing complexity, in order to allow participants to check, improve and assess their own modelling technique. In this paper, only the results obtained from spectral and pushover analyses are presented and used to conduct shear verifications according to normative requirements.

CASH-Phase 2 outcomes prove that today adequate tools for structural analysis are available, though they still have to be improved in order to optimize the nonlinear response prediction. On the other hand, there is a need for NLFEA guidelines (such as those published for static analyses by the Dutch Ministry of Public Works, [8]-[10]), to reduce modelling uncertanties.

2 Description of the analysed RC walls

The geometry of the two specimens (one regular and one irregular) is indicated in Fig. 1. The walls represent the facades of a NPP building with four floors and a total height of 16 meters. The total width of the walls is 12 meters and the thickness is 0.4 meters. Two 0.4 x 1.0 m side flanges simulate the presence of perpendicular walls in the NPP building, while 0.4x1.0 m beams simulate the RC diaphragm. The irregular wall differs from the regular one due to the absence of the shear wall on the level 2 at the second bay.

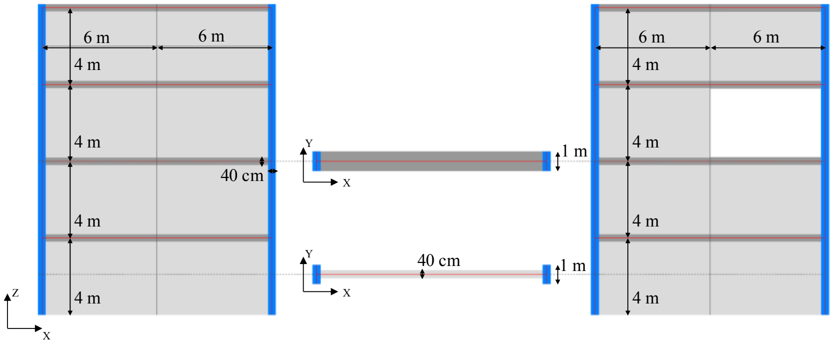

Fig. 1 Geometry description of regular and irregular wall.

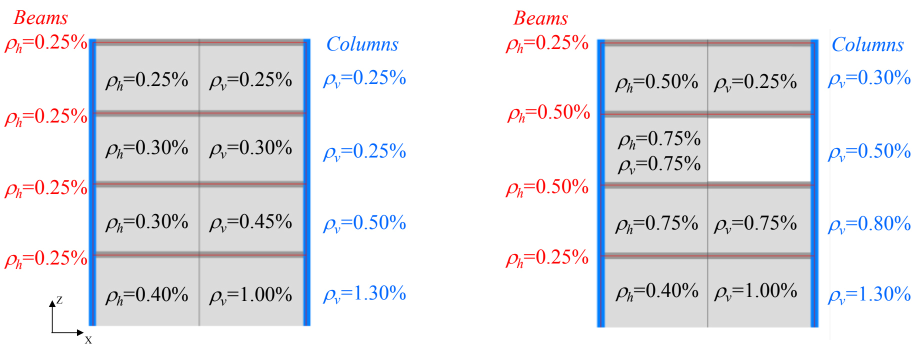

Fig. 2 Shear wall total reinforcement.

Table 1 Mechanical properties of materials.

Concrete					Steel			
f_c [MPa]	E_c [MPa]	f_t [MPa]	ν	ρ [kg/m^3]	f_y [MPa]	E_s [MPa]	E_h [MPa]	ρ [kg/m^3]
35.0	30000.0	2.0	0.2	2300.0	500.0	200000.0	1000.0	7500.0
E_c = modulus of elasticity of concrete f_c = cylinder compressive strength of concrete f_t = tensile strength of concrete ν = Poisson's coefficient					E_s = modulus of elasticity of steel E_h = hardening modulus of reinforcing steel f_y = yield strength of reinforcing steel ρ = material density			

The reinforcements ratio of beams, columns and walls are reported in Figure 2 and are obtained from the design study considering a determined seismic ground motion. Steel rebars are distributed symmetrically on both sides of each element (NECS [7]). Table 1 shows the mean values of concrete and steel mechanical properties. The loads consist of self-weight of structural elements, vertical masses applied on the floors to model the live loads (per floor M_z = 60 t) and horizontal masses applied on the floors to adjust the first horizontal frequency (per floor M_h = 500 t).

3 Structural response provision

3.1 Modelling strategies

The adopted FEM models are reported in Fig. 3. 864 nodes and 644 multi-layered shell elements, with average element size equal to 550 mm, have been used to model the walls. The analyses were conducted using the ABAQUS 6.12 software where the PARC_CL 2.0 crack model [1] is implemented in the UMAT.for subroutine. The Newton-Raphson method was adopted as convergence criterion.

The wall structures are clamped at the base and the out of plane displacements are prevented in all mesh nodes. The self-weight of structural members has been applied as density while the horizontal and vertical masses as lumped mass elements. The total mass in horizontal and vertical direction is 2248 t and 488t respectively.

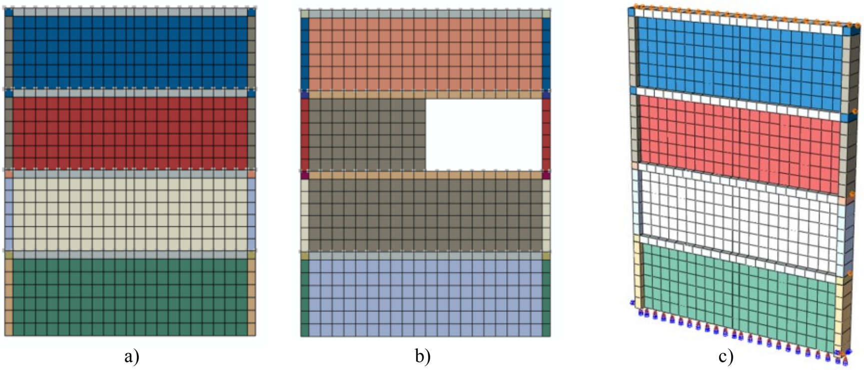

a) b) c)

Fig. 3 Finite element mesh of a) regular wall, b) irregular wall and c) elements shell thickness.

3.2 Modal spectral analysis

The linear response spectrum results of the walls are presented in Fig. 4 and Fig. 5. The analyses have been conducted with reduced Young modulus $E_c/2$ for concrete using the acceleration spectrum shown in Fig. 4a. Fig. 4b-c shows the first mode deflected shape for the regular and irregular walls having frequencies respectively equal to 4.03 Hz e 3.42 Hz.

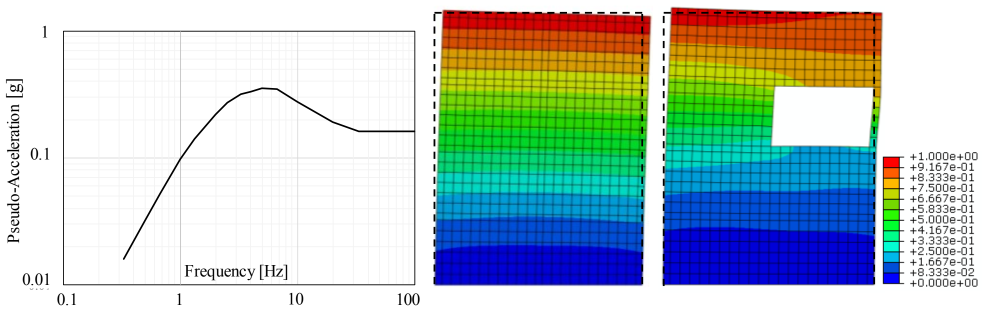

a) b) c)

Fig. 4 a) Elastic response spectrum and first mode deflected shape for b) regular wall and c) irregular wall.

Fig. **5** illustrates the diagram of the shear force, the bending moment and the inter-storey drift for the regular and the irregular wall, calculated with spectral analysis considering only the first vibration mode. Fig. **5**, highlights the substantial difference between the deformed shape of the irregular wall and the regular one due to the presence of the opening at level 2.

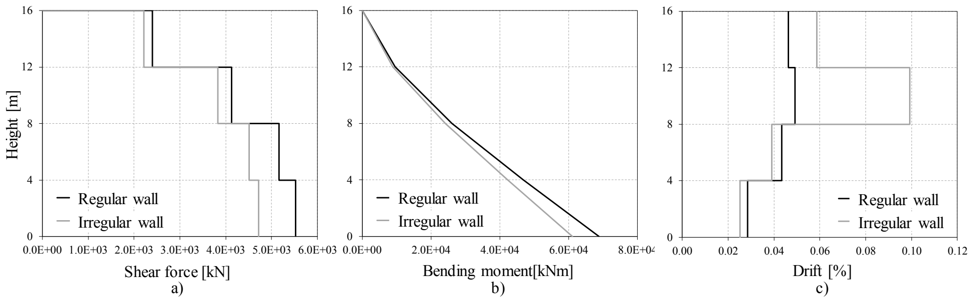

Fig. 5 a) Shear force, b) bending moment and c) inter-storey drift diagrams for the regular and irregular wall height obtained by spectral analysis.

3.3 Pushover analysis

The nonlinear pushover analyses have been conducted in load control applying a first mode proportional distribution of horizontal forces. The normalized force distribution at each level is (0.17, 0.43, 0.72, 1) for the regular wall and (0.11, 0.30, 0.75, 1) for the irregular wall. For the irregular wall, the pushover analysis was permormed in direction +X and –X. In Fig. 6 the shear base–top displacement curves (top displacement has been assumed equal to the displacement of P4B point indicated in Fig. 7) are shown. The capacity, in terms of resistance and ductility, of the irregular wall is lower than the capacity of the regular one because of the presence of the opening. The NLFEAs terminated after the reaching of the ultimate rebar strain equal to 4% and the ultimate concrete strain equal to 3.5‰.

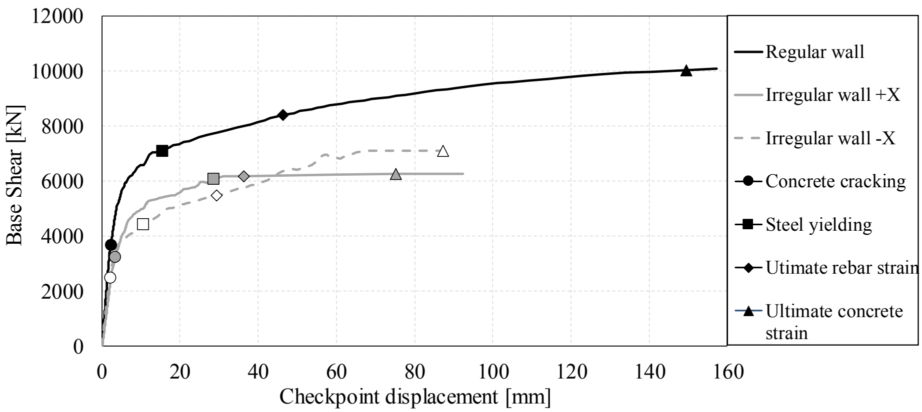

Fig. 6 Pushover analysis of regular and irregular walls.

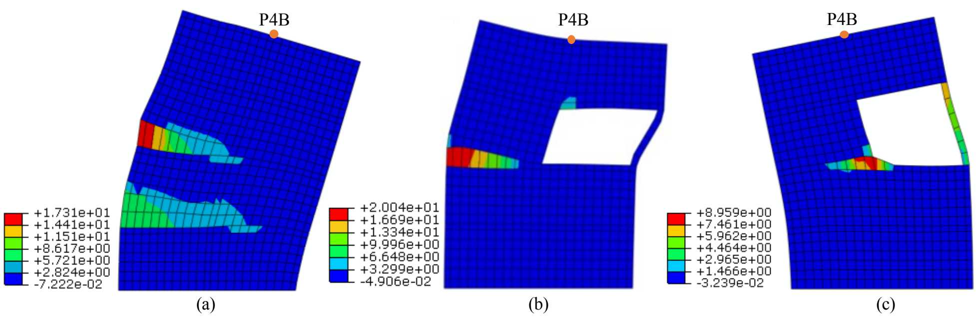

Fig. 7 Crack width [mm] obtained in correspondence of the ultimate concrete strain: (a) regular, (b) irregular +X, (c) irregular –X.

In Fig. 7 the contour plot of the crack width in correspondence of the reaching of the ultimate concrete strain is presented. The cracks appear particularly localized at the level 2 both for the regular and irregular wall. Furthermore, the irregular wall presents high values of crack width in correspondence of the opening.

4 VERIFICATION OF THE REGULAR WALL ACCORDING TO EUROCODE 8 DESIGN RULES

The verification of the regular wall has been performed in accordance with Eurocode 8 [11] rules for new structures and existing structures to verify if standard codes provisions are able to detect the actual failure mode with appropriate safety margins in case of multi-storey RC walls. Safety verifications have been performed using a linear model which is usually adopted in daily practice.

4.1 Verification according to design rules for new structures

The behavior factor q_0 of the wall has been derived from Eq.(1), according to Eurocode 8 [11] and results equal to 2.5:

$$\mu_\phi = 2q_0 - 1 \qquad if\ T_1 \geq T_C \tag{1}$$

where T_1 is the fundamental period of the building and T_C is the period at the upper limit of the constant acceleration region of the spectrum; μ_ϕ is the curvature ductility factor, equal to 6.19 and obtained from the bilinearization of the pushover analysis.

The design shear forces V_{Ed} is obtained in accordance with Eq.(2):

$$V_{Ed} = \varepsilon \cdot V_E \tag{2}$$

where ε is the shear magnification factor calculated using Eq.(3) which results equal to 2.5:

$$1.5 \leq \varepsilon = q \cdot \sqrt{\left(\frac{\gamma_{Rd}}{q} \cdot \frac{M_{Rd}}{M_{Ed}}\right)^2 + 0.1 \cdot \left(\frac{S_e(T_C)}{S_e(T_1)}\right)^2} \leq q \tag{3}$$

where γ_{Rd} is the factor to account for over strength due to steel strain-hardening; M_{Rd} is the design flexural resistance at the base of the wall; M_{Ed} is the design bending moment at the base of the wall; $S_e(T)$ is the ordinate of the elastic response spectrum.

Fig. 8 reports the seismic actions demand on RC wall, obtained from response spectrum analyses results and modified according to the capacity design approach, together with the RC wall capacities. Eurocode 8 [11] design procedure assumes that the plastic hinge has formed at the base of the wall, precluding plastic hinges in the upper stories and, for this reason, all shear forces along the entire height of the wall have to be multiplied by the shear magnification factor ε. In reality, the regular wall object of CASH-phase 2 benchmark, exhibited flexural failure at the level 2, as illustrated in Fig. 7. So to consider the development of plastic hinges at higher levels, Rutenberg [12] proposed a not uniform envelope of the shear forces over the building height as a function of the fundamental natural period T_1, Eq.(4). The comparison between the design shear force V_{Ed}, obtained using a uniform value of ε, and the design shear force obtained according to Rutenberg [12], $V_{Ed,Rutenberg}$, is shown in Fig. 8b.

$$\xi = 1 - 0.3 \cdot T_1 \geq 0.5 \tag{4}$$

The shear resistance has been evaluated according to the variable truss formulations currently adopted by Eurocode 2 [13] and Eurocode 8 [11]. The design value of the shear resistance, V_{Rd}, is the minor between the values given by Eq.(5) and Eq.(6) which respectively provide the design shear force which can be sustained by the yielding shear reinforcement, $V_{Rd,s}$, and the maximum shear force limited by crushing of the compression struts, $V_{Rd,max}$.

$$V_{Rd,s} = \frac{A_{sw}}{s} z \cdot f_{ywd} \cdot \cot\theta \tag{5}$$

where A_{sw} is the cross-sectional area of shear reinforcement, s is the spacing of the stirrups, f_{ywd} is the design yield strength of the shear reinforcement and z=0.9d, where d is the effective depth of the cross-section.

$$V_{Rd,\max} = \alpha_{cw} \cdot b_w \cdot z \cdot \nu_1 \cdot f_{cd} / (\cot\theta + \tan\theta) \tag{6}$$

where α_{cw} is a coefficient taking account of the state of the stress in compression chord, b_w is the minimum width between tension and compression chords, ν_1 is a strength reduction factor for concrete cracked in shear and f_{cd} is the design value of the concrete compressive strength.

From a collection of experimental evidence on RC walls comes a study published by Fardis [14] demonstrating that the shear resistance of RC walls reduces as the damage and therefore the ductility increases. For this reason, in Eurocode 8 [11] the design value of shear resistance, as controlled by diagonal compression failure of the web, Eq.(6), is taken as 40% of the value given by Eurocode 2 [13] in case of high ductility class (DCH).

Fig. 8a shows that the wall does not fail for bending because the flexural capacity M_{Rd} is higher than the demand M_{Ed} at each level. Fig. 8b demonstrates that the wall does not fail neither for shear. Indeed, the design shear demand calculated according to Eq.(2), V_{Ed}, and according to the demand shear distribution over the length, $V_{Ed,\ Rutenberg}$, is less than the design shear resistances calculated according to Eurocode 8 [11] both for medium ductility class (DCM), $V_{Rd,DCM}$, and for high ductility class, $V_{Rd,DCH}$. Fig. 8a reports, using a dashed grey line, the scaled flexural demand, $M_{Ed,scaled}$, which causes a flexural failure mode at level 2. On the basis of this scaled value, equal to 2.38, the shear demand has been recalculated according to Eq.(2) and the scaled shear demand, $V_{Ed,scaled}$, has been plotted in Fig. 8b using a dashed grey line. Fig. 8b shows that the amplification of spectral acceleration, considered on the basis of ductile flexural failure modes, causes an anticipated shear failure if the design shear resistance is calculated in case of high ductility class (DCH). Since the regular wall does not experience brittle shear flexural modes during NLFEA, it results that the coefficient equal to 0.4 (adopted to reduce the diagonal compression resistance) is too conservative. Contrarily, if the design shear resistance is calculated in case of medium ductility class (DCM) (without reducing the diagonal compression resistance), the expected failure mode, obtained using linear model and simplified verification, is in agreement with NLFEA outcomes.

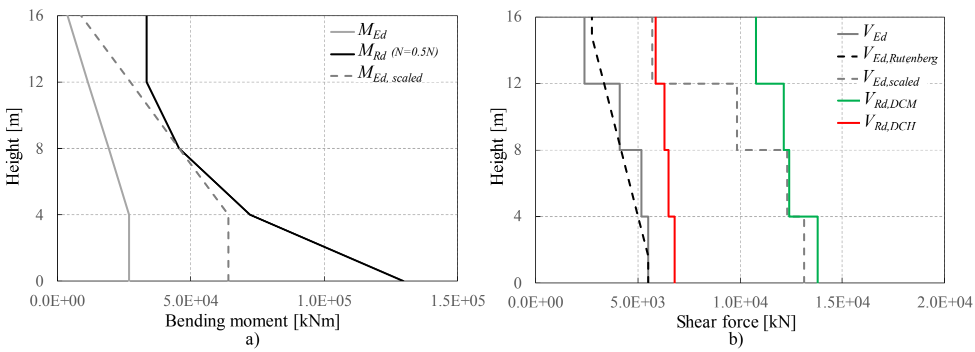

Fig. 8 a) flexural and b) shear verification obtained using design formulations adopted for new structures.

4.2 Verification according to Eurocode 8-part3 design rules for existing structures

To check the acceptability of the adopted linear model, the ratios $\rho_i = D_i/C_i$ values have been calculated at each level of the regular wall. The ductile demand has been calculated from linear response spectrum analysis while the flexural capacity has been calculated by assuming mean values of material strength.

Fig. 9a shows that, the capacity is higher than the demand for ductile mechanisms and ρ_i results lower than 1 at each level; therefore, the demand for brittle mechanism can be obtained from the analysis, as illustrated in Fig. 9b.

The capacity for brittle mechanisms is then calculated in terms of strength by using the mean values of properties divided by the confidence factor, *CF*, (equal to 1 in this case where a full knowledge, KL3, is assumed) and by the partial factor.

According to Eurocode8-part 3 [15] prescriptions for existing walls, the shear strength V_R, as controlled by the stirrups, is given by Eq.(7):

$$V_R = \frac{1}{\gamma_{el}}\left[\begin{array}{l}\frac{h-x}{2L_v}\min\left(N;0.55\cdot A_c f_c\right)+\left(1-0.05\min\left(5;\mu_\Delta^{pl}\right)\right)\cdot \\ \left[0.16\max\left(0.5;100\rho_{tot}\right)\left(1-0.16\min\left(5;\frac{L_v}{h}\right)\right)\sqrt{f_c}A_c+V_w\right]\end{array}\right] \tag{7}$$

where h is the depth of cross-section, x is the compression zone depth; N is the compressive axial force; $L_v=M/V$ is the ratio moment/shear at the end section; f_c is the mean values of the compressive strength of concrete, A_c is the cross-section area, taken as being equal to b_{wd} for a cross-section with a rectangular web of width (thickness) b_w and structural depth d; $\mu_\Delta{}^{pl}$ is the plastic part of the displacement ductility factor; ρ_{tot} is the total longitudinal reinforcement ratio; V_w is the contribution of transverse reinforcement to shear resistance.

The shear resistance of a concrete wall, V_R, may not be taken greater than the value corresponding to the web failure due to concrete crushing $V_{R,max}$, Eq.(8):

$$V_{R,\max} = \frac{0.85\left(1-0.06\min\left(5;\mu_\Delta^{pl}\right)\right)}{\gamma_{el}}\left(1+1.8\min\left(0.15;\frac{N}{A_c f_c}\right)\right)\left(1+0.25\max\left(1.75;100\rho_{tot}\right)\right)\cdot$$
$$\left(1-0.2\min\left(2;\frac{L_v}{h}\right)\right)\sqrt{f_c}b_w z \tag{8}$$

where z is the length of the internal lever arm.

Fig. 9a reports, using a dashed grey line, the scaled flexural demand, $M_{Ed,\mathrm{scaled}}$, which causes a flexural failure mode at level 2 and a ratio $\rho_i = D_i/C_i = 1$. The corresponding scaled response spectrum acceleration is therefore the maximum value for the evaluation of shear demand from spectral analysis, which results $V_{Ed,scaled}$ in Fig. 9b. Finally, Fig. 9b shows that in case of verification, in accordance with Eurocode 8-part3 design rules for existing structures, the analysed wall is not resulting a critical shear member and the expected failure mode is governed by ductile mechanisms at level 2 according to non-linear analyses outcomes.

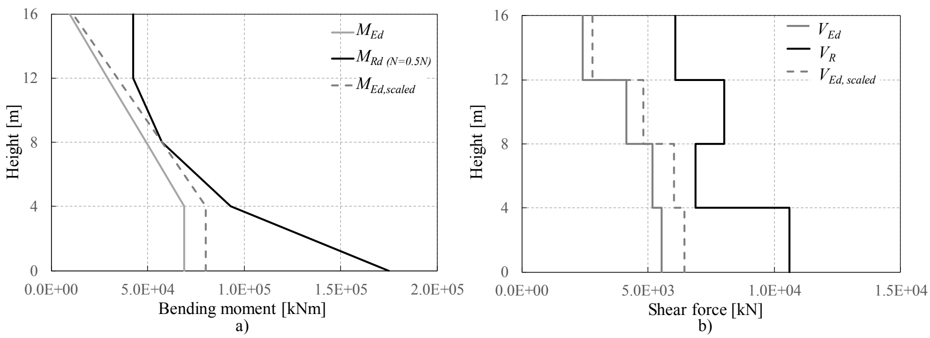

Fig. 9 a) flexural and b) shear verification obtained using design formulations adopted for existing structures.

5 Conclusions

In this paper the results of the CASH-phase 2 blind prediction obtained by the team of the University of Parma are illustrated. The non-linear response of multi-storey RC walls has been predicted using PARC_CL 2.0 crack model implemented in user subroutine UMAT.for of Abaqus software. The main outcome of the research presented in this paper are listed in the following:

- The response prediction of complex structures like multi-storey wall with and without opening can be reliably obtained using NLFE tools.
- The response prediction of complex structures, like multi-storey wall not exhaustively investigated via experimental tests, obtained from NLFEA could lead to un-expected failure mode and different capacity and ductility evaluation than assessments obtained from analytical formulations provided by standard codes (like Eurocode 8).

• In particular too conservative calculation of maximum compressive shear web resistance (adopted in case of high ductility class) could lead to un-safe verifications. Indeed, simplified approaches could cause an erroneous evaluation of the failure mode: for example for the analysed multi-storey walls it results governed by shear instead of by flexure.

• More sophisticated calculation methods can detect more realistic failure modes than expected with code like formulations and therefore more effective and optimized design strategies.

• Considerable efforts are still needed to understand the behavior of seismic-resisting wall systems. Normative prescriptions are often based on few experimental campaigns carried out on isolated elements. In order to better understand the non-linear behavior, numerical methods able to predict the response of seismic-resisting wall systems and their interaction with diaphragms and secondary structural elements are required hopefully supported by experimental evidences.

Acknowledgements

This paper reports on the scientific results obtained by the University of Parma within the PRIN project (Italian Research Project of Prominent National Interest): "Failure mechanisms due to lack of construction details and degradation phenomena in existing reinforced concrete buildings-Meccanismi di rottura per carenza di dettagli costruttivi e fenomeni di degrado in strutture in cemento armato esistenti" financially co-supported by MIUR (the Italian Ministry of Education, University and Research).

References

[1] Belletti B, Scolari M, and Vecchi F. 2017. “PARC_CL 2.0 crack model for NLFEA of reinforced concrete structures under cyclic loadings.” *Computers and Structures* 191:165–179. https://doi.org/10.1016/j.compstruc.2017.06.008.

[2] Belletti B, Muttoni A, Ravasini S, and Vecchi F. 2018. “Parametric analysis on punching shear resistance of reinforced concrete continuous slabs.” *Magazine of Concrete Research* 2018. doi: 10.1680/jmacr.18.00123.

[3] Abaqus 6.12. 2012. *User’s and Theory Manuals*. http://www.3ds.com/

[4] Damoni C, Belletti B, and Esposito R. 2014. “Numerical prediction of the response of a squat shear wall subjected to monotonic loading.” *European Journal of Environmental and Civil Engineering* 18(7):754-769.

[5] Belletti B, Stocchi A, Scolari M, and Vecchi F. 2017. “Validation of the PARC_CL 2.0 crack model for the assessment of the nonlinear behaviour of RC structures subjected to seismic action: SMART 2013 shaking table test simulation.” *Engineering Structures*. 150:759-773.

[6] Belletti B, Scolari M, and Vecchi F. 2017. “Simulation of monotonic, static and dynamic response of RC squat walls by means of PARC_CL 2.0 crack model.” COMPDYN 2017, Rhodes Island, Greece, June 15-17.

[7] N005_A469_2014_EDF_B. THECNICAL REPORT. “Presentation of the cash benchmarck phase 2.” http://benchmark-cash.org/

[8] Hendriks M.A.N, De Boer A, and Belletti B. 2017. “Guidelines for Nonlinear Finite Element Analysis of Concrete Structures.” Rijkswaterstaat Centre for Infrastructure, Report RTD:1016-1:2017.

[9] Belletti B, Damoni C, den Uijl J.A, Hendriks M.A.N, and Walraven J.C. 2013. “Shear resistance evaluation of prestressed concrete bridge beams: fib Model Code 2010 guidelines for Level IV approximations.” *Structural concrete* 14(3): 242-249

[10] Belletti B, Damoni C, Hendriks M.A.N, De Boer A. 2014. “Analytical and numerical evaluation of the design shear resistance of reinforced concrete slabs.” *Structural Concrete* 15(3): 317-330.

[11] EN 1998-1-8:2005. Eurocode 8: Design of structures for earthquake resistance.

[12] Rutenberg A, and Nsieri E. 2006. “The Seismic Shear Demand in Ductile Cantilever Wall Systems and the EC8 Provisions.” Bulletin of Earthquake Engineering 4:1-21.

[13] “EN 1992-1-1, 2002. Eurocode 2: Design of concrete structures. - Part1-1: General rules and rules for buildings.” 2004.

[14] Fardis M. “Seismic design assessment and retrofitting of concrete buildings.” Springer Ed 2009.

[15] “EN 1998-3:2005. Eurocode 8 - Design of structures for earthquake resistance - Part 3: Assessment and retrofitting of buildings”.